Modeling and Control of a Fuel Cell System in Transport Applications

Jérôme Lachaize, Maurice Fadel, Stéphane Caux, Pascal Schott, Laurent Nicod

MODELING AND CONTROL OF A FUEL CELL SYSTEM IN TRANSPORT APPLICATIONS

J.Lachaize*, M.Fadel*, S.Caux*, P.Shott, L.Nicod*****
**Laboratoire d'Electrotechnique et d'électronique industrielle, UMR, LEEI INPT ENSEEIHT, CNRS*
2 rue Camichel 31071 Toulouse cedex 7 France.
Tel : +33(0)5 61 58 82 08
lachaize@leei.enseeiht.fr ;fadel@leei.enseeiht.fr ; caux@leei.enseeiht.fr
***Laboratoire Hydrogène et Pile à Combustible, LHPAC,CEA/DTA/DEM/SPCM-17 rue des Martyrs*
38054 Grenoble cedex 9 France.
Tel: +33(0)4 38 78 48 40
pascal.schott@cea.fr
****ALSTOM Transport SA, 50 rue du docteur guinier BP 4- 65600 Séméac France.*
Tel : +33(0)5 62 53 48 57
laurent.nicod@transport.alstom.com

Abstract: This paper presents a Modeling approach to control the PEM fuel cell auxiliaries and the design of control laws. In a second time, we present the structure specification of an electrical power train with fuel cell for high power transport applications. This work shows that we can characterize and adjust the system control on an operating cycle with the simulation tools. *Copyright © 2003 LEEI INPT, UMR 5828, CNRS.*

Keywords: Modeling, Simulation, Control Methods, Real-Time Operation of Power Plants, non-conventional energy sources, distributed energy generation.

1- INTRODUCTION.

The use of fuel cell is now envisaged to supply electric energy in high power rail transport applications. So we realize a study to control the structure of the fuel cell system and the electrical chopper which composed the electric power train.

In a first time, we present the fuel cell model and its auxiliaries used to design the controllers. Then we explain the control strategy of these auxiliaries, only for air compressor and valve pressure.

In a second time, we detail the power train structure as well as the control scheme of each electrical chopper and first results of energy management.

2- GLOSSARY.

Fi	Molar flow.
N	Number of cells bystack.
F	Faradays constant 96485 C/mol.
I	Current in A.
l_{H_20}	Hydration rate of the membrane.
X_{0_2}	Molar fraction of 0_2 in air =21%
StO_2	Stochiometry rate of oxygen.
R	Molar gas constant. 8.13 J/K/mol.
V_{cath}	Cathodic Volume in m^3
T_{fc}	Temperature in Kelvin.
Pi	Pressure in Pascal.
Cyl	Compressor capacity in m^3.
ω	Rotation speed in rad/s.
γ	Polytropic exponent, for air γ=1.4.
M	Molar masse of air.

3- FUEL CELL SYSTEM.

The fuel cell system is composed by the fuel cell core associated with all the necessary auxiliaries for an embedded fuel cell system.

This schema represents all the functions present in a fuel cell system:

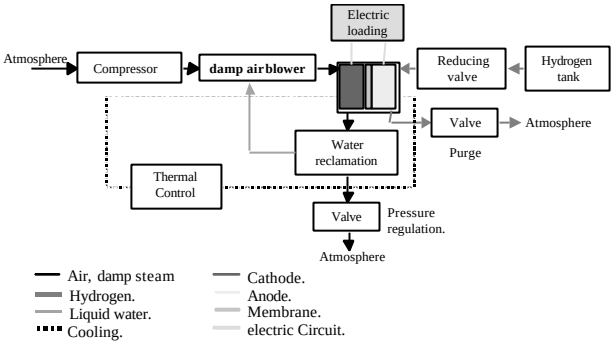

Fig 1. : Fuel cell system.

The Modeling process consists in writing the variations of the species concentrations, then in calculating the pressure in each compartment. After this step we use a quasi-static model to establish the voltage variation of the fuel cell [1] [2].

The nominal point of the system is:

$$P_{outlet} = 1\ 10^5\ Pa\ ;\ P_{inlet} = 1.6\ 10^5\ Pa\ ;\ T_{fc} = 353.15°K\ ;$$

$$StO_2 = 1.6\ ;\ Power\_nom = 400\,kW\ ;\ Unom_{\min} = 375V$$

4- FUEL CELL MODELING.

4.1- Cathodic species schedule.

These equations describe the variations of the gaseous species concentrations in the cathodic compartment.

The balance of oxygen and nitrogen allows us to write the following equation:

$$\begin{cases} \dfrac{dnO_2}{dt} = 0.21F_{in} - F_{O_2c} - X_{0_2}F_{valve} \\ \dfrac{dnN_2}{dt} = 0.79F_{in} - X_{N_2}F_{valve} \\ \dfrac{dn_{vap}}{dt} = \dfrac{X_{vap}}{1 - X_{vap}}F_{in} - X_{vap}F_{valve} \end{cases} \quad (1)$$

Where: $F_{O_2c} = \dfrac{NI_{fc}}{4F}$ $\quad X_{vap} = \dfrac{P_{sat}(T_{fc}°)}{P_{cath}}$ $\quad X_i = \dfrac{P_i}{P_{cath}}$

With :

– Fin inlet molar flow of the compressor.
– F_{valve} outlet molar flow of the valve.
– Xi molar fraction of i species .
– F_{O2c} oxygen molar flow consumed by the fuel cell.

4.2- Anodic species schedule.

In the anodic compartment, we can write the same type of balance.

$$\frac{dnH_2}{dt} = F_{H_2in} - F_{H_2c} - F_{H_2valve} \qquad F_{H_2c} = \frac{NI_{fc}}{2F} \qquad (2)$$

With :

– F_{H2in} inlet molar flow of the Reducing valve.
– F_{H2c} hydrogen molar flow consumed by the fuel cell.
– $F_{H2valve}$ outlet molar flow of the valve.

4.3- Pressure calculation.

We use the perfect law gases hypothesis to calculate the pressure:

$$P_{cath} = \frac{RT_{fc}}{V_{cath}}(n_{O_2} + n_{H_2} + n_{vap}) \qquad (3)$$

The dynamic model of the pressure variation is:

$$P_{cath} = \frac{RT_{fc}}{V_{cath}} \frac{1}{p}\left((1 + \frac{X_{vap}(P_{cath}, T_{fc})}{1 - X_{vap}(P_{cath}, T_{fc})}) F_{comp} - F_d \right) \qquad (4)$$

With: $F_d = F_{O2\,cons} + F_{valve}$

We can also calculate the partial pressures:

$$P_{O_2} = \frac{RT_{fc}}{V_{cath}} n_{O_2} \qquad P_{H_2} = \frac{RT_{fc}}{V_{cath}} n_{H_2} \qquad (5)$$

4.4- Voltage calculation.

The voltage variations of the fuel cell are computed with a quasi-static model, because the chemical reaction dynamic is faster than the system dynamics.

This voltage depends on the current density in the fuel cell, the partial pressures (of hydrogen and oxygen), the temperature of the reaction, and the hydration of the membrane. $Ufc = f(I, PO_2, PH_2, T_{fc}, l_{H_2O})$

Hypothesis of the model:

– Insignificant Anodic activation voltage.
– Uniform current density.
– Uniform temperature.

The voltage expression is:

$$Ufc = E_{Nernst} - \frac{RT_{fc}}{2aF} \ln\left(\frac{j}{j_o}\right) - R_{mem}\, j - j\left(c\,\frac{j}{j_{\max}}\right)^2 \qquad (6)$$

With :

– α= symmetry factor (0,5).
– j_o = current exchange.j_0=[10^{-7}A/cm^2;10^{-5}A/cm^2].
– R_{mem}=f(T_{fc},λ_{H2O}) membrane resistance (0,162 Ω/cm^2).
– j_{max}=2.5A/cm^2 maximum current.
– c=0.471 coefficient due to simplification.

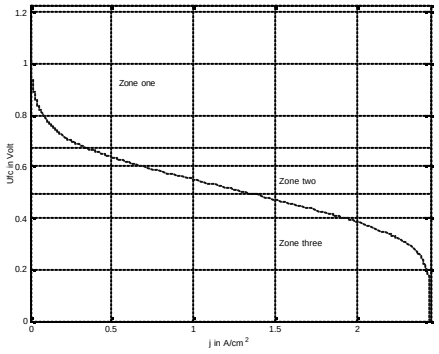

Fig 2. : Polarisation curve.

In the polarisation curve, we can see three zones:

- Cathodic activation (zone one) : $\frac{RT_{fc}}{2a\,F} \ln\left(\frac{j}{j_o}\right)$.
- Ohmic loss (zone two) : $R_{mem}\, j$.
- Diffusion limitation (zone three) : $j(c\, j / j_{\max})^2$.

The Nernst law is valid on all the voltage range. This law represents the voltage of the oxidation-reduction reaction :

$$E_{Nernst} = \frac{\Delta G^0}{2F} + \frac{RT_{fc}}{2F} \ln\left(\frac{P_{O_2}}{10^5} \frac{P_{H_2}}{10^5} \right) \qquad (7)$$

5- COMPRESSOR MODELING.

After Modeling the PEM core, we must study the air supply process to obtain the dynamics of the voltage developed by the fuel cell.

The air supply system of the fuel cell is composed by a screw type compressor. We choose this type of compressor to avoid the flow oscillations and the lubrication. The rotation is made by a synchronous drives with permanent magnets.

NB: we work here on a low-pressure fuel cell system.

5.1- Outlet flow compressor.

The outlet flow is detailed in [3] and is:

$$q_{molar} = \frac{P_{outlet}}{RT_{outlet}} Cyl \frac{w}{2p} h_v \qquad (8)$$

The volumetric efficiency h_v allows us to include several phenomena in the model:

- The total mechanical clearances between rotor and compressor casing .
- Compression rate.
- Rotor peripheral speed.
- Flow density.

The volumetric efficiency depends on the rotor speed and compressor rate ($tx = \frac{P_{outlet}}{P_{inlet}}$) as seen on fig 3.

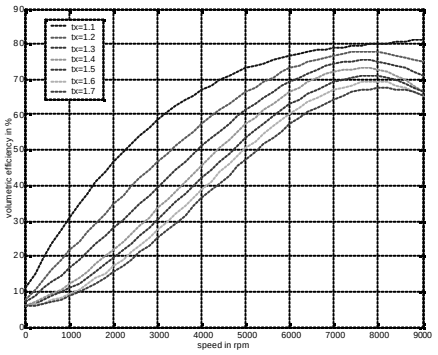

Fig 3. : Volumetric efficiency.

5.2- Flow simplification modeling.

The association of the synchronous machine (with speed control) and the compressor can be represented by the following diagram:

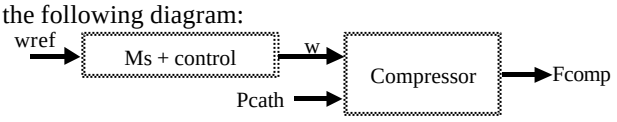

Fig 4. : Synchronous machine and compressor.

From this functional diagram we can write the evolution law of the compressing flow *'Fcomp'*. We place upstream speed reference an inverse model of the compressor in order to have a linear relation between the variable of entry *'e'* and the flow of the compressor *'Fcomp'*.

The inverse model is representing by the following maps on Matlab:

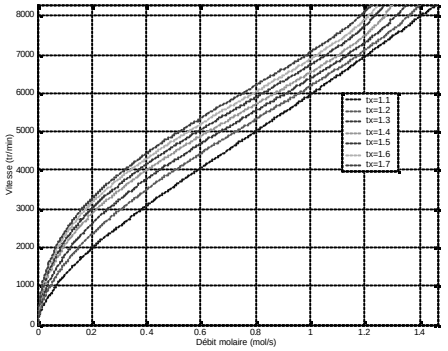

Fig 5. : compressor inverse model.

Therefore, we can write the following diagram:

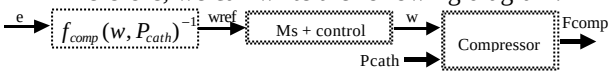

Fig 6. : flow modeling.

The synchronous engine and its controller are equivalent to a first order system. So the exit flow of the compressor is represented by:

$$F_{comp} = \frac{1}{p}\left(\frac{1}{t}e - \frac{1}{t}F_{comp}\right) \qquad (9)$$

6- VALVES MODELING.

The molar flow of the valves is expressed in function of the opening section, the temperature, and the outlet and inlet pressures [4]:

$$F_{valve} = S_{open}\sqrt{\frac{2P_{inlet}^{2}}{MRT_{inlet}}\frac{g}{g-1}\left(\frac{P_{outlet}}{P_{inlet}}\right)^{\frac{2}{g}} - \left(\frac{P_{outlet}}{P_{inlet}}\right)^{\frac{g+1}{g}}} \qquad (10)$$

This valve models is linearized around the nominal point. So the new model is: $F_{valve} = S_{open}K_{valve}$

7- AUXILIARY CONTROL STRATEGY

7.1- Steady state modeling.

Therefore, the modelisation of the fuel cell system result in a two states model [2][5]where:

$$X = [\mathrm{Pcath}\ \mathrm{Fcomp}]^{t}$$

$$\dot{X} = \begin{bmatrix} 0 & (1+\frac{X_{vap}(P_{cath},T_{fc})}{1-X_{vap}(P_{cath},T_{fc})})\frac{RT_{fc}10^{-5}}{V_{cath}} \\ 0 & -\frac{1}{t} \end{bmatrix} X + \begin{bmatrix} -\frac{RT_{fc}10^{-5}}{V_{cath}} & 0 \\ 0 & -\frac{1}{t} \end{bmatrix} \begin{bmatrix} Fd \\ e \end{bmatrix}$$

In this modelisation the pressure is in bar.

The nonlinear model is linearized around the nominal point. So we can write :

$$\dot{X} = \begin{bmatrix} 0 & (1+\frac{X_{vap_n}}{1-X_{vap_n}})\frac{RT_n10^{-5}}{V_{cath}} \\ 0 & -\frac{1}{t} \end{bmatrix} X + \begin{bmatrix} -\frac{RT_n10^{-5}}{V_{cath}} & 0 \\ 0 & -\frac{1}{t} \end{bmatrix} \begin{bmatrix} Fd \\ e \end{bmatrix} \qquad (11)$$

7.2- Feedback Control Design.

The system controller is implemented in digital so we numerize the steady state. The sampling frequency is equal to: $fe = 166\,Hz$

The new steady state is:

$X(k+1) = A_d X(k) + B_d u(k)$ and $Y(k) = C_d X(k)$

The control structure schema is:

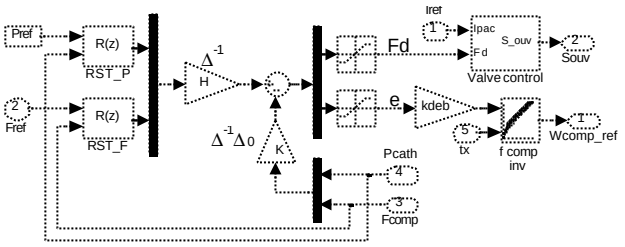

Fig 7. : Pressure and flow control.

In order to create uncoupling of the two states variables we write:

$$u(k) = \Delta^{-1}v(k) - \Delta^{-1}\Delta_0 X(k) \qquad (12)$$

With: $\Delta = B_d$ and $\Delta_0 = A_d$

with this steady state feedback the new system is simplified as: $P_{cath} = z^{-1}v_1$ *and* $F_{comp} = z^{-1}v_2$.

After uncoupling the system we implement RST regulator in order to control the two variables with different dynamics.

The regulator structure is:

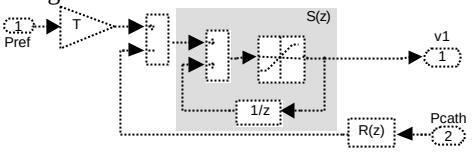

Fig 8. : Pressure and flow regulator.

Where:

$$S(z^{-1}) = 1 - z^{-1}; \qquad R(z^{-1}) = r_0 + r_1 z^{-1}; \qquad T = R(1) \qquad (13)$$

The polynomial regulator coefficients are calculated by the pole placement. The chosen characteristic polynomial of the close loop is.

$$P(z^{-1}) = 1 + p_1 z^{-1} + p_2\ z^{-2} = (1 - z^{-1}\exp(-w\,Td))^{2} \qquad (14)$$

with:

$w = 15\,rad/s$ for pressure loop.

$w = 50\,rad/s$ for flow compressor loop.

We obtain:

$$r_0 = p_1 + 1 \; and \; r_1 = p_2 \qquad (15)$$

The flow reference is calculated with the Faradays law:

$$F_{ref} = \frac{N\,I\,St_{O2}}{4F\,X_{0_2}} \qquad (16)$$

7.3- Simulation results.

This simulation represents the evolution of pressure and flow when power is requested on fuel cell. It is realized with a very complete model on simulink.

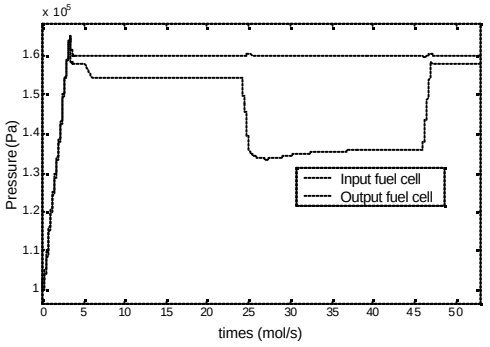

Fig 9. : Cathodic pressure.

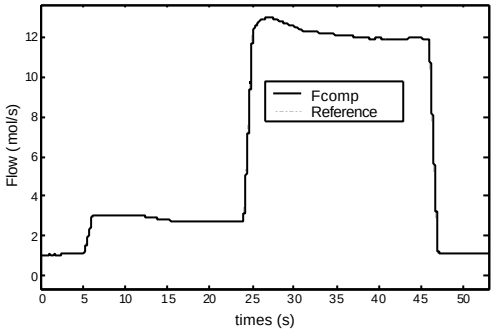

Fig 10. : Compressor flow

As we can see on this simulation the pressure is remained constant despite the compressor flow variation. We can also see that the compressor flow tracks the flow reference.

8- TRACTION CHAIN.

8.1- Architecture.

The fuel cell is now, connected to the DC link with an electronic chopper. The existing fuel cell sub-system has to be designed for high power and does not exist for the moment. That is why an Energy Storage System (ESS) must be associated with the fuel cell. In addition the ESS is able to absorb the braking energy of the vehicle. The ESS technology chosen is supercaps. This ESS is connected to the DC link by another electronic chopper.

Both sources must give the power demand by the propulsion motor and the auxiliaries of the vehicle. The electrical choppers are connected by parallel structure as shown on fig 11.

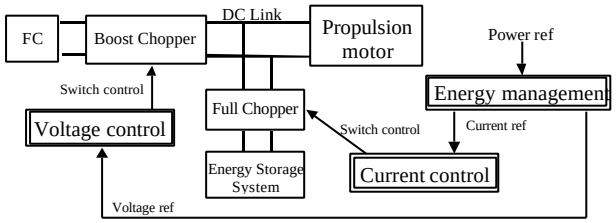

Fig 11. : Power Train and control structure.

The fuel cell chopper is a Boost because in the high power rail transport applications the voltage of the Dc link is high. This chopper is controlled for the DC link voltage regulation. So a loop voltage regulation is used.

The supercaps full chopper is a Buck/Boost because this chopper must be reversible in current. This chopper is in current regulation control mode to manage the charge and discharge of the ESS. The current reference is computed in function of the ESS power reference which is obtained by an energy strategy.

8.2- Boost Modeling and Control

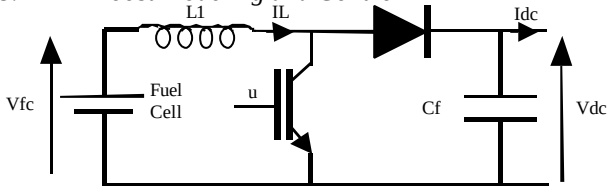

Fig 12. : Boost principle schema.

$\{L1 = 0.95mH \text{ and } Cf = 3.2mF\}$

The power switch is control by PWM with α duty cycle. The constant frequency is fd=1/Td .With the PWM control. Chopper is described by the following average model.

$$\begin{cases} Vfc = L_1 \dfrac{dIL}{dt} + (1-a)Vdc \\ IL(1-a) = Cf\, \dfrac{dVdc}{dt} + Idc \end{cases} \quad (17)$$

This chopper is controlled for the DC link voltage regulation. In the aim to have good control of the voltage we have realized two regulation loops : one on the current and an other one on the voltage[6]. To obtain suitable transfer function for control purpose, we realized a linearization by an inverse model. So we write:

$$a = \frac{VL'-Vfc}{Vdc} + 1 \quad (18)$$

With this linearization the current model is:

$$T_1(p) = \frac{Il(p)}{VL'(p)} = \frac{1}{L_1\, p} \quad (19)$$

To implement a digital controller we numerize the transfer function, the sampling frequency is equal to the switch frequency.

$$H(z^{-1}) = \frac{B(z^{-1})}{A(z^{-1})} = \frac{Td}{L_1}\frac{z^{-1}}{(1-z^{-1})} \quad (20)$$

Finally we establish a classical sampled regulation structure (Fig. 13) with an RST regulator with these polynomials corresponding to proportional and integrator controller:

$$S(z^{-1}) = 1 - z^{-1}; \quad R(z^{-1}) = r_0 + r_1 z^{-1}; \quad T = R(1) \quad (21)$$

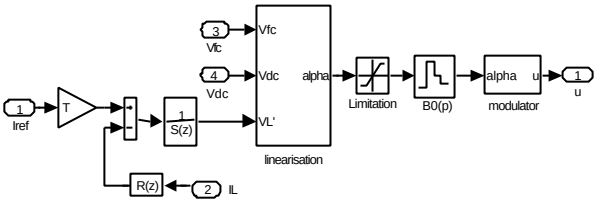

Fig 13. : Boost current loop.

The regulation coefficients are calculates by the pole placement. The characteristic polynomials of the closed loop is.

$$P(z^{-1}) = 1 + p_1 z^{-1} + p_2\, z^{-2} = (1 - z^{-1}\exp(-w\,Td))^2 \quad (22)$$

with: $w = 2pfd/10 = 3142\ rad/s$.

We obtain:

$$\begin{cases} r_0 = \dfrac{L_1}{Td}(p_1 + 2) \\ r_1 = \dfrac{L_1}{Td}(p_2 - 1) \end{cases} \quad (23)$$

In order to avoid windup we have implemented an anti-windup structure in the regulation loop.

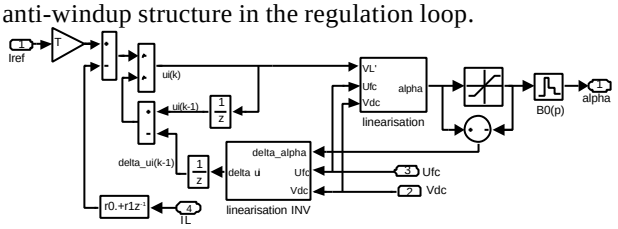

Fig 14. : Boost current loop implementation.

In the same way, to add a voltage control loop, we realised a linearisation by an inverse model with:

$$Iref = \frac{Vdc}{Vfc}(Iref' + Idc) \quad (24)$$

So we can write the voltage model:

$$T_2(p) = \frac{Vdc(p)}{Iref'(p)} = \frac{1}{Cf\, p} \quad (25)$$

We have here the same type of transfer than in the voltage loop so we made the same digital controller with also an anti-windup.

The structure of this controller is show in fig 15:

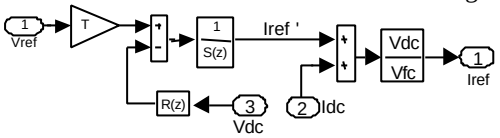

Fig 15. : Boost voltage loop.

The coefficient of the regulation are.

$$\begin{cases} r_0 = \dfrac{Cf}{Te}(p_1 + 2) \\ r_1 = \dfrac{Cf}{Te}(p_2 - 1) \end{cases} \quad (26)$$

Here we have the same characteristic polynomials with: $w = 2pfd/100 = 314\,rad/s$.

8.3- Buck/Boost Modeling and Control.

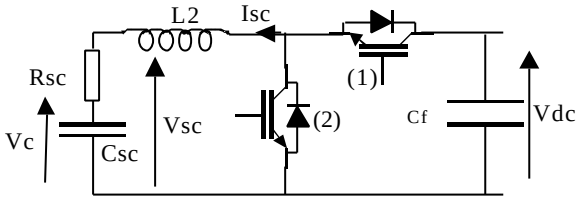

Fig 16. : Buck/Boost principle schema.

$$\{L2 = 0.94mH\,;\, Cf = 3.2mF\,;\, rsc = 55m\Omega\,;\, Csc = 47F\}$$

This chopper is described by the following average model which allows us to establish the equation in the two working phases[7].

Differentials equations in Buck case :

$$\frac{disc}{dt} = \frac{1}{L_2} Vdc\; a_1 - \frac{Rsc}{L_2} isc - \frac{Vc}{L_2} \; and \; \frac{dVc}{dt} = \frac{isc}{Csc} \quad (27)$$

Differentials equations in Boost case :

$$\frac{disc}{dt} = \frac{1}{L_2} Vdc\,(1 - a_2) - \frac{Rsc}{L_2} isc - \frac{Vc}{L_2} \; and \; \frac{dVc}{dt} = \frac{isc}{Csc} \quad (28)$$

In order to simulate this chopper we write:

$$Vpwm = a_1 Vdc\; Buck/Boost + (1 - a_2)\, Vdc\; \overline{Buck/Boost} \quad (29)$$

Where Buck/Boost binary variable represents the type of the chopper operation. This chopper control is of course a current regulation to manage the charge and discharge of the ESS. In order to have one model and one regulator we write that the control in the boost mode is the complement of the control in the Buck mode. In this case the Boost model can be wrote as a Buck model. But in the control loop we must compute the complement value of the rate cycle when the Boost operation is activated. The current transfer function is:

$$T(p) = \frac{Isc}{a} = \frac{CscVdc\; p}{1 + Rsc\,Csc\; p + L_2\, Csc\; p^2} \quad (30)$$

The DC link voltage is constant because this voltage is control by the Boost chopper.

To implement a digital controller we numerize the transfer function, the sampling frequency is equal to the switch frequency.

$$H(z^{-1}) = \frac{B(z^{-1})}{A(z^{-1})} = \frac{b_1 z^{-1}(1 - z^{-1})}{1 + a_1 z^{-1} + a_2 z^{-2}} \quad (31)$$

We establish a sampled regulation structure as on fig 17. We compute an RST regulator with these polynomials:

$$S(z^{-1}) = 1 - z^{-1}\,;\, R(z^{-1}) = r_0 + r_1 z^{-1}\,;\, T = \frac{A(1) + b_1 R(1)}{b_1} \quad (32)$$

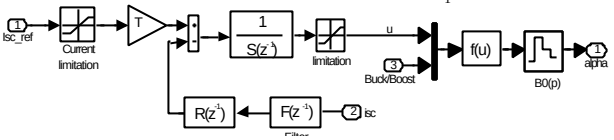

Fig 17. : Buck/Boost current loop.

The function in the f(u) bloc is the implemented function to calculate the complement value of the α rate cycle when the Boost operation is activated. So we write:

$$alpha = u\; Buck\;/\;Boost + (1 - u)\overline{Buck\;/\;Boost} \quad (33)$$

The type of the chopper operation variable (Buck/Boost) is calculated by:

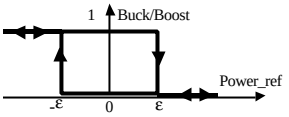

Fig 18. : Buck/Boost operation.

This is simulated by a relay because the zeros value of the current must be in the two modes because the chopper can make a current with a zero average value. So we have:

Buck mode when Buck/Boost=1.

Boost mode when Buck/Boost=0.

The balance point of this converter is for the average current equal to zero. When the chopper is in one mode we have an intermittent flow for little value of the current. The first solution in order to control the chopper is to hold the mode to the last active mode and to filter the current. The second solution is to switch between the both mode when we have zero current. We have decided to implement the first solution so we filter the supercaps current by a numerical Butterworth (5 orders) filter $F(z^{-1})$. The regulation coefficient are calculated by the pole placement.

$$\begin{cases} r_0 = (p_1 - a_1)/b_1 \\ r_1 = (p_2 - a_2)/b_1 \end{cases} \quad (34)$$

The characteristic polynomials is:

$$P(z^{-1}) = 1 + p_1 z^{-1} + p_2\; z^{-2} = (1 - z^{-1} \exp(-w\,Td))^2 \quad (35)$$

Where: $w = w_{fil}/10 = 1500\,rad/s$ and w_{fil} is the angular frequency cutting of the filter.

Due to current overshoot when the chopper operation changed, we must initialised the duty cycle at each changed to set the current to zero.

The initialised value is: $a_{init} = Vsc/Vdc$

The implementation structure of the loop regulation with initialisation and anti-windup is:

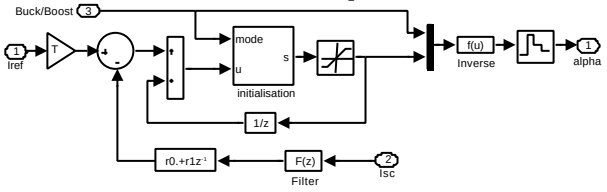

Fig 19. : Current regulation implementation.

The initialization is computed by the structure seen on fig 16:

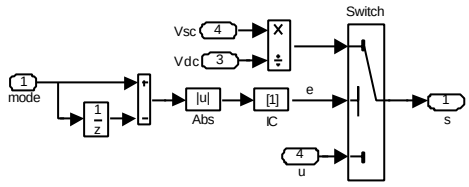

Fig 20. : Initialization computed.

The initialization structure detect the mode modification and put the control variable to the init value. The current reference is calculated in function of the ESS power reference and the loses estimation of the chopper. The power reference is provided by an energy strategy.

In Buck case :

$$ESS\ \ power\ \ ref\,(k) = Power\ \ ref\,(k) - Losses\,(k-1) \qquad (36)$$

In Boost case :

$$ESS\ \ power\ \ ref\,(k) = Power\ \ ref\,(k) + Losses\,(k-1) \qquad (37)$$

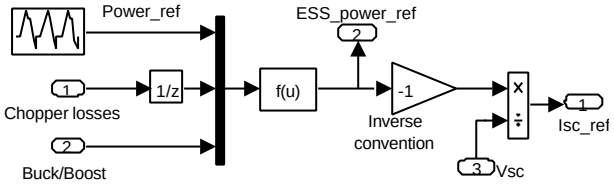

Fig 21. : Current reference.

The current reference is also managed by a logical function in order to limit the supercaps voltage (in max and min value). The losses of the chopper are estimated in average value by a value plant[8][9].

8.4- Simulation results.

The aim of this simulation in average value is to view some responses of the main system variables. Data used for the power reference are taken from ADVISOR (NREL software) simulation.

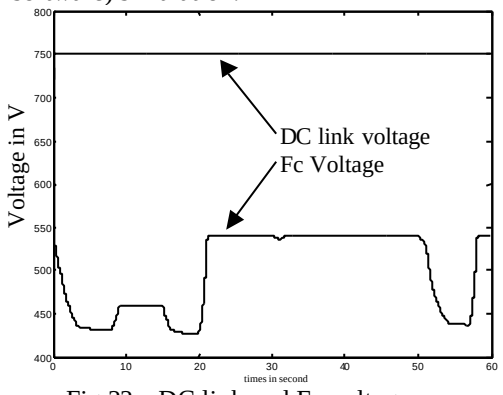

Fig 22. : DC link and Fc voltage

We can see that the first converter has a voltage regulation and this voltage remained constant despite the power request on the DC link.

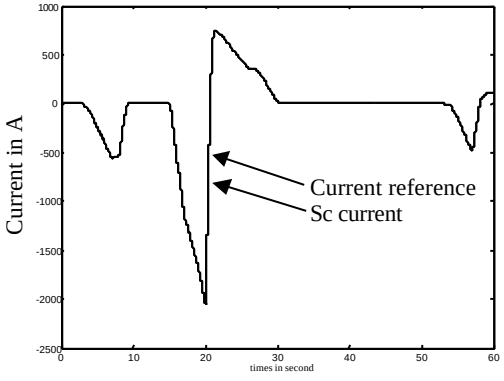

Fig 23. : Desired and real current

The simulation shows also that the second chopper has a current regulation and the current in the supercaps tracks the current reference. We can also see that this chopper is reversible in current.

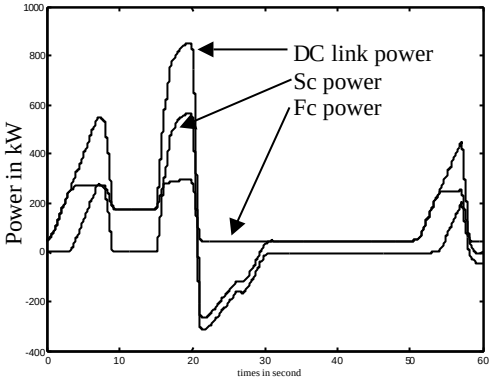

Fig 24. : power traction on an operating cycle.

As we can see on this simulation, the power of the propulsion motor and auxiliaries is separated between the fuel cell and the supercaps following the energy management chosen. The quasi-static model seems to be sufficient for the power train simulation but, we are now testing if we must develop a dynamic model of the fuel cell.

9- CONCLUSION.

In order to control the fuel cell system we develop the fuel cell model, the air compressor model, and the valves model. We have only developed in this paper the control structure of the air supply system and pressure valves. But in the fuel cell system, there are other auxiliaries to control, like the cooling system. So we must continue the study on the control structure.

10- REFERENCES.

[1] W Friede, S Raël, B Davat: “PEM fuel cell models for supply of an electric load”, proc of Electrimacs 2002, August 18-19.

[2] Jay T.Pukrushpan, Anna G.Stefanopoulou, Huei Peng: “Modeling and Contol for PEM Fuel Cell Stack System”, proc of the American Contol Conference – Anchorage, Michigan - May 8-10-2002.

[3] VARAIX corporation documentation: “Compressor efficiency definitions” and “ Evaluation of vairex air system technology for automotive fuel cell power systems (fcps) “: website www.vairex.com

[4] Bird, Stewart, light foot: book: “Transport Phenomena" p481, Wiley international edition, ISBN: 0-471-07395-4

[5] Wiartalla Andreas, Lang Olivier, Pischinger Stefan, Schönfelder Carter: “Efficiency Boosting of Fuel Cell System Considering Part Load Operation”, proc of FISITA 2001 World Automotive Congress -Helsinki, Finland – June 2-7-2002

[6] M.Fadel :”Lois de commande pour une alimentation AC/DC à absorption de courant sinusoïdal”, proc of 3EI 2000.

[7] B.J.Arnet, L.P.Haines: “High Power DC-to-DC Converter For Supercapacitors”, proc of IEMDC 2001 – Boston, Massachusetts.

[8] International Rectifier documentation: “Application characterisation of IGBT’s” : website: www.irf.com/technical-info/an990/an-990.htm

[9] EUPEC corporation data-sheet: “ EUPEC :FZ 1600 R 17 KF6 B2” : website www.eupec.com